# Thioester synthesis through geoelectrochemical CO2 fixation on Ni sulfides

**Norio Kitadai** ( nkitadai@jamstec.go.jp )
Japan Agency for Marine-Earth Science and Technology
**Ryuhei Nakamura**
Earth-Life Science Institute, Tokyo Institute of Technology
**Masahiro Yamamoto**
Japan Agency for Marine-Earth Science and Technology
**Satoshi Okada**
Japan Agency for Marine-Earth Science and Technology https://orcid.org/0000-0001-5417-5955
**Wataru Takahagi**
Japan Agency for Marine-Earth Science and Technology
**Yuko Nakano**
Tokyo Institute of Technology
**Yoshio Takahashi**
University of Tokyo
**Ken Takai**
Japan Agency for Marine-Earth Science and Technology https://orcid.org/0000-0003-4043-376X
**Yoshi Oono**
University of Illinois at Urbana Champaign

**Article**

**Keywords:** Autotrophic Metabolism, Origin of Life, Early Ocean Hydrothermal Systems

**Posted Date:** August 31st, 2020

**DOI:** https://doi.org/10.21203/rs.3.rs-66151/v1



**Version of Record:** A version of this preprint was published at Communications Chemistry on March 17th, 2021. See the published version at https://doi.org/10.1038/s42004-021-00475-5.

# Thioester synthesis through geoelectrochemical $CO_2$ fixation on Ni sulfides

Norio Kitadai[1,2*], Ryuhei Nakamura[2,3], Masahiro Yamamoto[1], Satoshi Okada[1], Wataru Takahagi[1,4], Yuko Nakano[2], Yoshio Takahashi[5], Ken Takai[1], and Yoshi Oono[6]

[*]Corresponding Author
Norio Kitadai: nkitadai@jamstec.go.jp
Tel.: +81-46-867-9708, Fax: +81-46-867-9715

[1]Super-cutting-edge Grand and Advanced Research (SUGAR) Program, Institute for Extra-cutting-edge Science and Technology Avant-garde Research (X-star), Japan Agency for Marine-Earth Science and Technology (JAMSTEC), 2-15 Natsushima-cho, Yokosuka 237-0061, Japan.
[2]Earth-Life Science Institute, Tokyo Institute of Technology, 2-12-1 Ookayama, Meguroku, Tokyo 152-8550, Japan.
[3]Biofunctional Catalyst Research Team, RIKEN Center for Sustainable Resource Science, 2-1 Hirosawa, Wako, Saitama 351-0198, Japan.
[4]Department of Chemistry, Graduate School of Science, The University of Tokyo, 7-3-1 Hongo, Bunkyo-ku, Tokyo 113-0033, Japan.
[5]Department of Earth and Planetary Science, Graduate School of Science, The University of Tokyo, 7-3-1 Hongo, Bunkyo-ku, Tokyo 113-0033, Japan.
[6]Department of Physics, University of Illinois at Urbana-Champaign, 1110W. Green Street, Urbana, IL 61801-3080, USA (retired).

**Submitted to *Communications Chemistry***

## Abstract

Thioester synthesis by CO dehydrogenase/acetyl-CoA synthase is among the most ancient autotrophic metabolisms. Although the preceding prebiotic $CO_2$ fixation routes to thioesters are often suggested, none has any experimentally supported evidence. Here we demonstrate that, under an electrochemical condition realizable in early ocean hydrothermal systems, nickel sulfide (NiS) gradually reduces to $Ni^0$, while accumulating surface-bound CO due to $CO_2$ electroreduction. The resultant partially reduced NiS facilitates thioester (S-methyl thioacetate) formation from CO and methanethiol even at room temperature and neutral pH. This thioester formation can further be enhanced up to a selectivity of 56% by NiS coprecipitating with FeS or CoS. Considering the central role of Ni in the enzymatic process mentioned above, our demonstrated thioester synthesis with the partially reduced NiS could have a direct implication to the autotrophic origin of life.


## Introduction

Thioester synthesis via acetylation of coenzyme A is a universal metabolic strategy of energy and carbon conservation. Molecular phylogenetics suggests that this biological reaction already functioned in the last universal common ancestor with carbon monoxide dehydrogenase (CODH) and acetyl-CoA synthase (ACS) as the prime catalysts.[1] At the Ni-based active centers bridged to an (or multiple) Fe−S cluster(s), CODH reduces $CO_2$ to CO using electrons typically taken from hydrogen ($H_2$), whereas ACS reacts CO with a methyl group to form acetyl, transferring it to CoA to form acetyl-CoA. These enzymatic processes often remind us of their prebiotic origins in a hydrothermal vent environment rich in $CO_2$, $H_2$, and (Fe,Ni)S minerals on the Hadean ocean floor.[2,3] Alternatively, a recent experimental work suggested a one-pot pyruvate synthesis from $CO_2$ and $H_2$ on an iron oxide ($Fe_3O_4$) and an iron-nickel alloy ($Ni_3Fe$) as a protometabolic reaction.[4] The proposed reaction, however, provides no explanation for the origin and antiquity of thioester-dependent metabolism. Thioesters possibly played rather central roles in protometabolism not only as carbon sources but also as energy currencies in a manner analogous to ATP,[5] serving as an entry point of phosphate into metabolism.[3]

However, nonenzymatic realization of the CODH/ACS reactions remains an experimental challenge. The $CO_2$-to-CO reduction requires a highly reducing potential that is inaccessible by the $H^+/H_2$ redox couple in the absence of flavin-based electron bifurcation (Figure S1).[6] In the ACS catalytic cycle, the active Ni site serves as both the electron donor and accepter through changing its oxidation state between +1 and +3, facilitating both the reduction and oxidation intermediate steps.[7] Such redox bifunctionality of Ni has never been observed in natural Ni-bearing minerals. Although

Huber and Wächtershäuser demonstrated S-methyl thioacetate (MTA) synthesis from CO and methanethiol in the presence of NiS as a potential prebiotic precursor of the ACS reaction,[8] the yield was very low (0.2% based on the initial amount of CO) even under their optimum condition (pH 1.6 and 100ºC), which is uncommon in nature.

How were $CO_2$-to-CO reduction and CO conversion realized under primordial realistic conditions? A clue is an *on-site* observation by Yamamoto et al.[9] of electricity generation in deep-sea hydrothermal vent chimneys and mineral deposits. The geoelectricity arises from the redox coupling between hydrothermal fluid chemicals and seawater-dissolved species via electrically conducting yet thermally insulating sulfide rocks (Figure S1).[10,11] Considering cool (0–50 ºC) and slightly acidic (pH 6–7) character of the ancient seawater,[12] together with pH and temperature dependences of the $H^+/H_2$ and $CO_2$/CO redox potentials,[13,14] $H_2$-rich alkaline hydrothermal systems must have readily provided negative electric potentials favorable for the $CO_2$-to-CO reduction at the chimney-ancient seawater interface. We previously demonstrated efficient $CO_2$ electroreduction to CO on some metal sulfide catalysts (for example, cadmium sulfide) under a simulated early ocean geoelectrochemical condition.[15] It was later found that FeS undergoes day-scale electroreduction to $Fe^0$.[16] The resultant FeS-$Fe^0$ assemblage, named FeS_PERM (FeS partially electroreduced to metal), showed exceptional capability of promoting various prebiotically important reactions owing to synergy between surface Fe sites with different oxidation states ($Fe^{2+}$ and $Fe^0$).[17,18]

In our previous works,[15,16] NiS exhibited neither CO evolution nor $Ni^0$ formation detectable by X-ray diffraction (XRD) analysis. However, our further investigation presented below found non-crystalline growth of $Ni^0$ under geochemically feasible potential conditions, with a substantial amount of CO bound on the resultant surface $Ni^0$ sites. It is furthermore shown below that the partially reduced NiS, that is, NiS_PERM realizes efficient conversion of CO and methanethiol to MTA even at room temperature and neutral pH. Notice that the accumulation of surface-bound CO during $CO_2$ electroreduction is generally recognized as a poisoning of surface (electro)catalytic activity,[19,20] but our results suggest that the CO accumulation process on NiS_PERM was rather a crucial step for subsequent primordial thioester formation in early ocean hydrothermal systems. Thioesters are versatile compounds in organic chemical synthesis as well as in biosynthesis, enabling diverse coupling reactions including C-C bond formation, esterification, and amide bond formation owing to the activated acyl unit.[21–23] To the best of our knowledge, our study provides the first experimental demonstration of thioester synthesis from CO and thiol under mild aqueous condition. Thus, besides rendering a realistic support for autotrophic scenarios of the origin of life,[2,3] our demonstrated CO-thiol reaction on NiS_PERM could be a practical approach to CO utilization.[24]

# Results

## Metal sulfide electroreduction

We prepared metal sulfides including NiS by simply mixing an aqueous solution of the corresponding metal chloride and an aqueous solution of sodium sulfide. The obtained sulfides were exposed to a constant electric potential for 7 days in 100 mM NaCl at room temperature (25 ± 2°C) under continuous $CO_2$ bubbling that maintained the solution pH at 6± 0.25 (Figures S2 and S3). The electrolyzed sulfides were then separated from the supernatant solution, dried under vacuum, and used for the following experiments.

The NiS consists of aggregated nanoparticles with an average particle diameter of 15 ± 11 nm (Figure S6). Although no significant morphological change was caused (Figure S6), exposure at –0.5 $V_{SHE}$ (volt versus the standard hydrogen electrode) led to the desulfurization of NiS to heazlewoodite ($Ni_3S_2$) (Figure 1a), consistent with thermodynamic calculation (Figure 1b). Further reduction of $Ni_3S_2$ at lower electric potentials was indicated by energy dispersive X-ray spectroscopy (EDS) mapping on the NiS particles electrolyzed at –1.0 $V_{SHE}$ (Figure 1c), where a clear decrease in the sulfur signal intensity relative to nickel was observed in comparison with pure NiS, and with the NiS electrolyzed at –0.5 $V_{SHE}$ (Figure 1d). In agreement with the EDS result, nickel K-edge X-ray absorption near-edge structure (XANES) of the NiS samples showed spectral changes with decreasing potential from –0.5 to –1.0 $V_{SHE}$ (Figure 1e) attributable to the occurrence and growth of $Ni^0$ in $Ni_3S_2$ up to the $Ni^0$ percentage of 12% at –1.0 $V_{SHE}$ (Figure 1f and Figure S11). Similarly, XANES analysis allowed us to estimate 7% conversion of CoS to $Co^0$ at –1.0 $V_{SHE}$ (Figure S12). Thus, NiS_PERM and CoS_PERM are formed at –1.0 $V_{SHE}$ and even less negative potentials near their sulfide/metal equilibria (Figure 1b and f, Figures S11 and S12) just as in the FeS case. However, in contrast to FeS that exhibited broad but clear XRD signals for $Fe^0$ even at –0.7 $V_{SHE}$ (Figure S8),[16] NiS showed no XRD signal for $Ni^0$ in the examined potential range (≤–1.0 $V_{SHE}$) (Figure 1a). The $Ni^0$ percentage up to 12% (Figure 1f) is well above the detection limit of XRD (Figure S10) if the formation of meso- or macroscopic crystalline structure is assumed. Thus, NiS_PERM would be with more finely dispersed zerovalent metal than FeS_PERM.

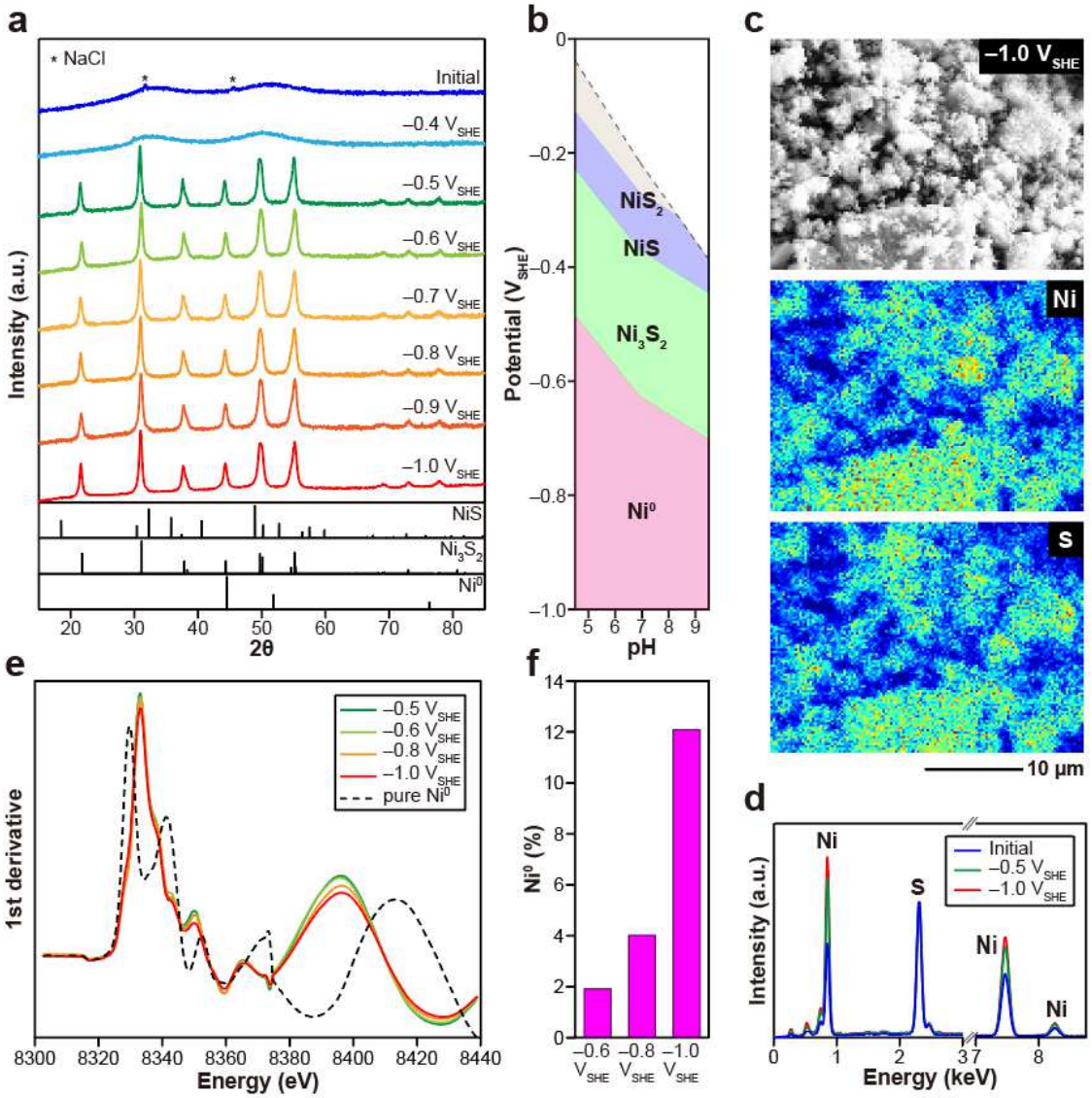


**Fig. 1. | NiS electroreduction characterized by (a) XRD patterns, (b) thermodynamic calculation, (c and d) SEM-EDX mapping data, and (e and f) nickel K-edge XANES spectra. (c)** presents the EDX mapping data for the NiS electrolyzed at –1.0 $V_{SHE}$. In **(d)**, the S signal intensities (2.3 keV) for NiS before (blue) and after the electrolysis at –0.5 $V_{SHE}$ (green) or –1.0 $V_{SHE}$ (red) are matched with each other for comparison. **(e)** The first derivative XANES spectra is shown.



131

## CO production and accumulation on the metal-sulfide PERMs

To explore the possibility of CO production and accumulation on the metal-sulfide PERMs formed under $CO_2$ atmosphere, we dissolved the resultant metal-sulfide PERMs completely in 35% hydrogen chloride, and quantified the released CO by gas chromatography (Figure S18 and Movie S1). Except for FeS, all the sulfides exposed at ≤–0.6 $V_{SHE}$ were found to retain CO (Figure 2a and Table S2). The threshold potential is close to the sulfide/metal equilibrium potentials for Ni and Co (–0.57 $V_{SHE}$ for both; Figure 1b and Figure S4), and is also near the thermodynamic $CO_2$/CO redox potential at the condition of sulfide electrolysis (–0.50 $V_{SHE}$; Figure S1). The amount of CO increased with decreasing the potential, up to 180 ± 40 μmol $g^{-1}$ for the case of NiS. Because sulfurized Ni binds CO considerably more weakly than pure $Ni^0$,[25] the observed CO should mostly derive from the CO bound on the surface $Ni^0$ sites. In fact, the maximum adsorption (180 ± 40 μmol $g^{-1}$) corresponds to the surface coverage of one CO molecule per 8 ± 3 surface Ni atoms (Figure S13), consistent with the percentage of $Ni^0$ grown at –1.0 $V_{SHE}$ (Figure 1f). The similar interpretation should be applicable to the adsorption behavior of CO on the CoS_PERM.[26] Coprecipitation with FeS led to decline of the amounts of CO on NiS and CoS (Figure 2a) probably because of the decrease in the surface reactive sites.

## Nonenzymatic thioester synthesis

We mixed the metal-sulfide PERMs retaining the surface-bound CO (Figure 2a) (50 mg for each) with an aqueous solution of sodium methanethiolate (75 μmol) in a serum bottle (13.8 ml), and agitated at room temperature (25 ± 2°C) for up to 7 days without externally imposing electric potential. pH was buffered at neutral (7.0 ± 0.5) by filling the gas space with $CO_2$ (1 atm). Despite this very mild condition, gas chromatograph–mass spectrometry analysis revealed efficient MTA formation in the presence of specific electrolyzed sulfides (Figure 2b and c). Organosulfur compounds detected with the amount higher than 0.01 μmol were methanethiol, MTA, dimethyl sulfide and dimethyl disulfide (Figures S19 and S20), among which MTA was the sole product built from CO and methanethiol:

$$CO + 2CH_3SH \rightarrow CH_3COSCH_3 + H_2S \qquad (1)$$

Experiments with the NiS_PERM prepared at –1.0 $V_{SHE}$ exhibited the following product characteristics. The yield of MTA increased over one week, while the amounts of CO and methanethiol decreased from their maxima at the beginning (Figure S24). CO appeared in the gas-

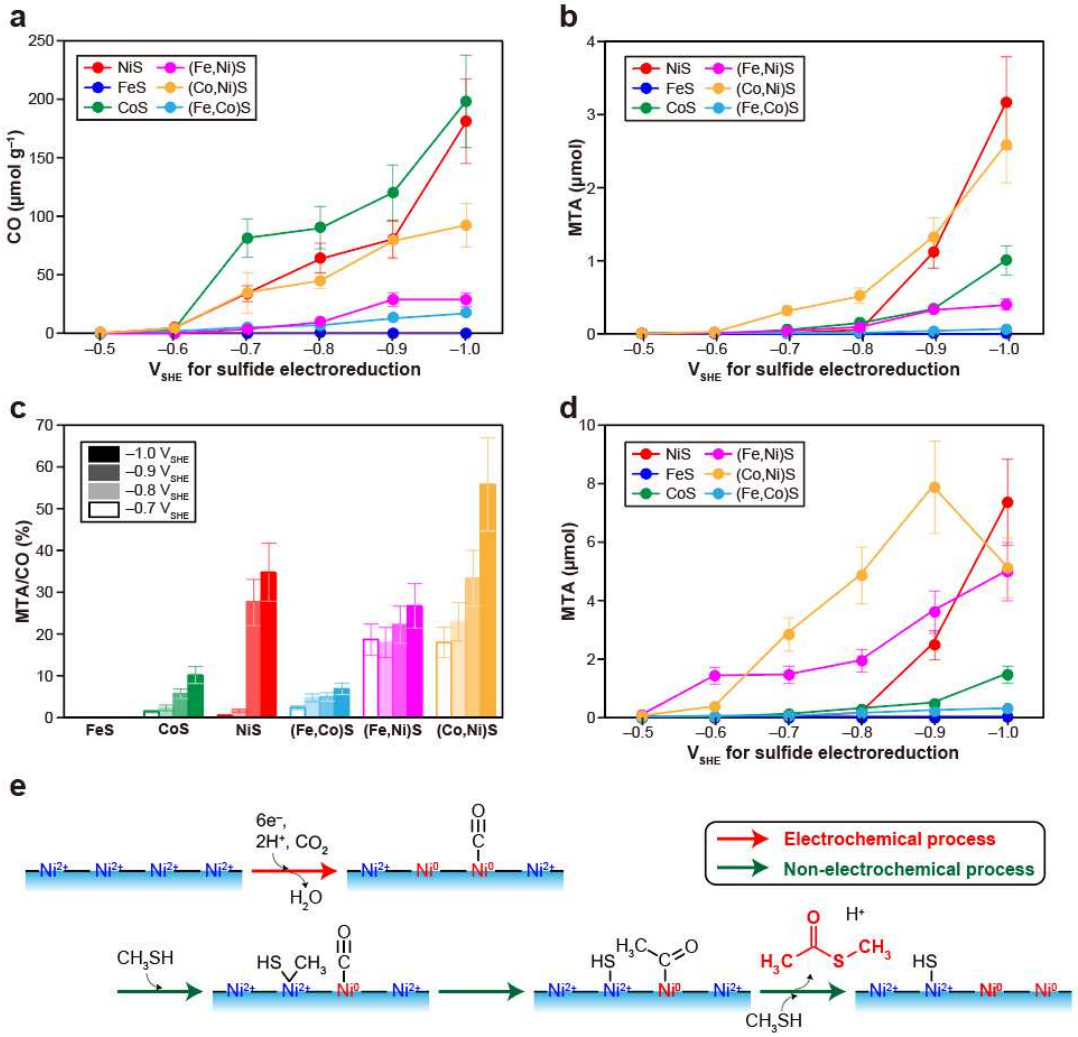


**Fig. 2. | CO accumulation through $CO_2$ electroreduction (a) and CO conversion to S-methyl thioacetate (MTA) (b–d) on the metal-sulfide_PERMs.** The surface-bound CO on the electrolyzed sulfides were quantified (a) and used as a carbon source for the MTA synthesis in the presence of methanethiol (75 μmol per 50 mg of sulfide) (b). The percentages of CO to form MTA are shown in (c). (d) The MTA synthesis were examined with CO and methanethiol externally added (75 μmol for each). The yield of MTA on (Co,Ni)S declined at the lowest potential (–1.0 $V_{SHE}$) because of depletion of methanethiol (Table S4). (e) Possible intermediate steps in the MTA formation via the formation of NiS_PERM with the surface-bound CO (red arrow) and the CO-methanethiol reaction on NiS_PERM (green arrows).



163

phase through competitive adsorption with methanethiol: in the absence of methanethiol under otherwise identical condition, few CO gas was detected (0.03 μmol) and no MTA was observed (Figure S21a). As long as methanethiol was available, replacement of $CO_2$ in the gas space with helium (He), and dissolution of 1 M phosphate (pH 7.0) into the sample solution had no significant influence on the yield of MTA (3.2 ± 0.6 μmol; Figure 2b → 3.6 ± 0.7 μmol). It was also confirmed with $^{13}$C-labeled $CO_2$ that the $CO_2$ filled in the serum bottle did not serve as a component of MTA. The MTA formed under $^{13}CO_2$ atmosphere showed the mass spectrum identical to that of the standard MTA with normal carbon isotopic composition.

In aqueous solutions, acetate (0.19 ± 0.04 μmol or 0.25 ± 0.05 mM) and formate (0.03 ± 0.01 μmol or 0.035 ± 0.01 mM) were observed (Figure S25). The acetate concentration increased to 2.0 ± 0.4 mM when the product solution was basified by 1 M sodium hydroxide due to MTA hydrolysis. Because MTA hydrolysis is accelerated at elevated temperatures,[27] a one-day experiment at 80°C resulted in a higher yield of acetate (2.4 ± 0.5 μmol or 3.2 ± 0.6 mM) and a lower yield of MTA (0.68 ± 0.14 μmol) (Figure S25). Other biologically relevant organic acids such as pyruvate and lactate were not detected in any product solutions with concentrations higher than 0.01 mM. We also treated solid samples with 8 M potassium hydroxide after the reaction, but neither pyruvate nor lactate was observed.

When CO, as well as methanethiol, were initially introduced with equal amounts (75 μmol, or 0.14 bar in the gas space) in the presence of NiS_PERM formed at –1.0 $V_{SHE}$, the yield of MTA more than doubled, compared with the case without CO in the initial gas phase (3.2 ± 0.6 → 7.4 ± 1.5 μmol; Figure 2d and Figure S21a). In contrast, under the same initial condition with CO, few or no detectable MTA was formed in the presence of pure NiS, the $Ni_3S_2$ prepared at –0.5 $V_{SHE}$, or pure $Ni^0$ (Figure S21 and Table S4), indicating the necessity of the coexistence of zerovalent and non-zerovalent Ni surface sites for efficient MTA production. It is also notable that the MTA yield decreased steeply as the NiS electroreduction potential was positively changed from –1.0 to –0.8 $V_{SHE}$ (Figure 2b to d) although –0.8 $V_{SHE}$ is still sufficient for the $Ni^0$ generation (Figure 1f). In light of reported chemical functions of Ni and other metals in organometallic analogues of ACS,[28,29] one possible interpretation is that the MTA synthesis involves at least two adjacent surface $Ni^0$ sites (Figure 2e): one $Ni^0$ serves as an electron donor for the reductive cleavage of methanethiol C-S bond. Close location of another $Ni^0$ (the closest Ni-Ni distance = 2.48 Å; Figure S13) allows transfer of the generated electrophilic methyl onto the nucleophilic carbon of adsorbed CO. After the formation of C-C bond to make the acetyl-$Ni^0$, its oxidative thiolysis to form MTA occurs through coupling with the reduction of neighboring non-zelovalent Ni atoms. The cleavage of methanethiol C-S bond also accounts for the

formations of $CH_4$ and dimethyl sulfide (Table S3 and S4), where the resultant methyl converts to $CH_4$ via protonation, while thiolysis of the methyl generates dimethyl sulfide. If a random $Ni^0$ distribution is assumed, a 12% conversion of $Ni^{2+}$ to $Ni^0$ achieved at –1.0 $V_{SHE}$ (Figure 1f) results in 1.4% occurrence of the adjacent $Ni^0$–$Ni^0$ surface pair, while this percentage drops to 0.16% with a 4% conversion achieved at –0.8 $V_{SHE}$. Thus, our proposed process taking multiple Ni sites into account (Figure 2e) explains the large potential dependence in MTA productivity of NiS_PERM (Figure 2b to d) as well as the few or no MTA formation on $Ni_3S_2$ and pure $Ni^0$, although this mechanism is different from the ACS-reaction. This nonenzymatic process is expected to be eventually deactivated due to cumulative surface sulfurization (Figure 2e), but the surface activity may be restored by additional solid electrolysis.

Interestingly, even greater CO-to-MTA reaction efficiencies were obtained with the NiS coprecipitating with FeS or CoS (Figure 2c). Up to 56 ± 10% of the surface-bound CO, produced by $CO_2$ electroreduction, was converted to MTA on the electrolyzed (Co,Ni)S. (Fe,Ni)S produced a considerable amount of MTA from initially introduced CO and methanethiol even after the –0.6 $V_{SHE}$ electrolysis (Figure 2d). Given FeS's electroreduction reactivity higher than that of NiS (Figures 7 and 8), Fe in the electrolyzed (Fe,Ni)S possibly assists the Ni's performance as an electron donor at an intermediate reduction step. The Fe's supportive role is also seen in the ACS-reaction as the form of ferredoxin serving as the redox mediator.[7] Co is also involved in the enzymatic process as a transporter of the methyl group.[7]

## Discussion

Our experiments revealed that partial electroreduction product of NiS, that is, NiS_PERM, promotes thioester synthesis from CO and methanethiol. NiS_PERM accumulates surface-bound CO during the formation under $CO_2$ atmosphere, so NiS offers a two-step $CO_2$ fixation route to thioester with the aid of electric energy. Ancient seawater was rich in $Ni^{2+}$ owing to much greater mantle activity than the present level.[30] Because $Ni^{2+}$ is almost insoluble in alkaline sulfide condition, Ni-bearing sulfides must have precipitated at the vent-seawater interface in early ocean alkaline hydrothermal systems, and has been exposed to a sustained negative potential by the geoelectrochemical processes (Figure S1). The potential level required for the $Ni^0$ formation and the surface-catalyzed CO production (≤–0.6 $V_{SHE}$; Figures 1 and 2) is attainable under moderately hot, $H_2$-rich, and alkaline conditions as observed even in the present-day hydrothermal systems.[31] The surface-bound CO is stable in NaCl aqueous solution, but is largely and quickly released in the presence of adsorption competitors such as methanethiol and hydrogen sulfide (see Materials and

Methods, Figures S26 and S27). Thus, considering dynamic mixing of hydrothermal fluids with seawater observed in the present-day deep-sea vent chimneys through the pore systems,[32] continuous CO production, concentration, desorption, and advection are likely to have occurred within the pore spaces of ancient hydrothermal mineral deposits (Figure 3). Such fluid-mediated materials transport favors the occurrence and combination of multiple reactions including the formation of thiols from CO (or $CO_2$) and $H_2S$,[33,34] the reaction of CO with methanethiol to form MTA (Fig. 2b to d), and the accumulation of organic products.[35] Thus, the thioester synthesis via the formation of Ni sulfide_PERMs should have been robustly concomitant with ubiquitous hydrothermal activities on the primordial seafloor.–

Nowadays, growing consensus for $CO_2$ as the dominant carbon species on the Hadean Earth has stimulated exploration of geo- and astro-chemical events that could have transiently realized highly reducing early atmosphere.[36] Subsequent photochemical and aqueous-phase processes with reactive carbon sources, powerful oxidizing/reducing agents, and/or UV light might have realized abiotic thioester synthesis. [37,38] Although these reactions might have played a role in enrichment of a prebiotic soup, their relevance to biosynthesis is ambiguous. Consequently, numerous questions

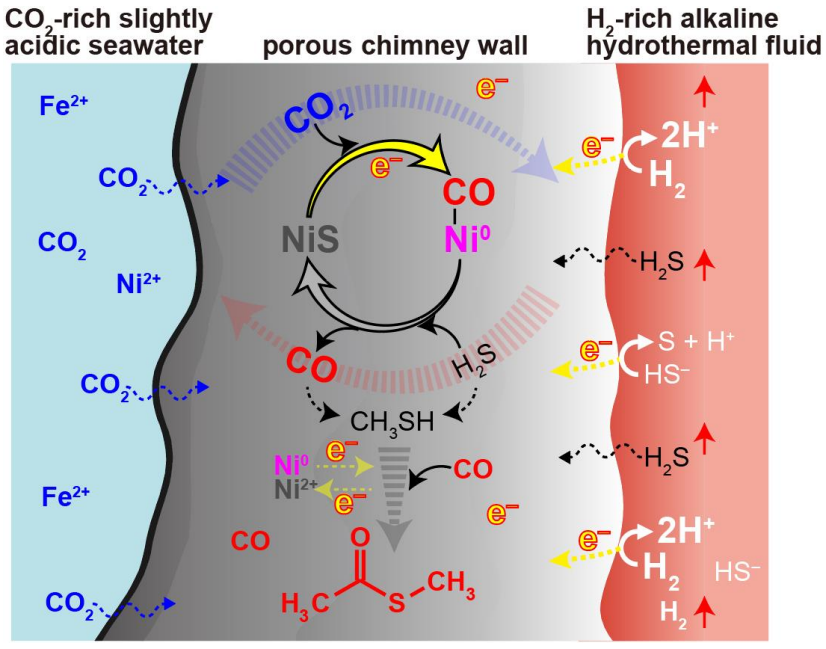


**Fig. 3 | Schematic cross-section of a vent chimney in an early ocean alkaline hydrothermal system showing possible abiotic thioester synthesis promoted by Ni sulfide_PERM.**

remain unanswered by the transient scenario regarding the gap between prebiotic chemistry and early biochemistry conserved in the metabolic and phylogenetic architectures of life.

The two key facts: $CO_2$ fixation utilizing various states of Ni due to our experiments (Figure 2) and the well-known central role of Ni at the active sites of CODH/ACS[7] may lead to a plausible scenario for the emergence of protometabolism prior to the origin of life. Sustained occurrence of electrochemical energy adequate for the Ni sulfide_PERM formation, $\leq$–0.6 $V_{SHE}$ in the ancient seawater condition (Figures 1 and 2), is limited in nature except for deep-sea hydrothermal settings (Figure S1). This environmental specificity with the known necessity of Ni in both biological and chemical $CO_2$ fixation suggest that the Ni sulfide_PERM-promoted thioester synthesis in early ocean hydrothermal systems (Figure 3) is a primordial precursor of the CODH/ACS reaction. The CO production on metal-sulfide_PERMs (Figure 2a) may also have served as crucial carbon and energy sources for the early chemolithotrophic ecosystem, thereby supporting, or even directing, the origin and early evolution of autotrophs as suggested from the autotrophic metabolism core.[39]


## Acknowledgements

We thank Reiko Nagano and Atsuko Fujishima for their help in laboratory experiments.


## Author contributions

N.K and Y.O. conceived the whole project based on the principled approach [40] and N.K. realized nonenzymatic thioester synthesis. Y.T. measured XANES spectra of the sulfide samples. S.O. performed SEM-EDX analysis, and W.T. prepared figures for the SEM-EDX data. N.K. performed all experiments except for the XANES and SEM-EDX measurements with technical support of Y.N., and prepared all figures and tables for the obtained results. S.O. considered possible intermediate steps in the MTA formation. All authors contributed to writing the paper.

## Competing interests

Authors declare no competing interests.

## Data availability

All data needed to evaluate the conclusions in the paper are present in the paper and/or the Supplementary Information. Additional data related to this paper may be requested from the authors.

## References


[1] Adam, P. S., Borrel, G. & Gribaldo, S. Evolutionary history of carbon monoxide dehydrogenase/acetyl-CoA synthase, one of the oldest enzymatic complexes. *Proc. Natl. Acad. Sci. USA* **115**, E1166–E1173 (2018).

[2] Russell, M. J. & Martin, W. The rocky roots of the acetyl-CoA pathway, *TRENDS Biochem. Sci.* **29**, 358–363 (2004).

[3] Sousa, F. L. et al. Early bioenegetic evolution. *Phil. Trans. R. Soc. B.* **368**, 20130088 (2013).

[4] Preiner, M. et al. A hydrogen-dependent geochemical analogue of primordial carbon and energy metabolism. Nature Eco. Evol. 4, 534–542 (2020).

[5] Goldford, J. E., Hartman, H., Smith, T. F. & Segre, D. Remnants of an ancient metabolism without phosphate. *Cell* **168**, 1126–1134 (2017).

[6] Schuchmann, K. & Müller, V. Autotrophy at the thermodynamic limit of life: a model for energy conservation in acetogenic bacteria. *Nature Rev. Microbiol.* **12**, 809–821 (2014).

[7] Can, M., Giles, L. J., Ragsdale, S. W. & Sarangi, R. X-ray absorption spectroscopy reveals an organometallic Ni–C bond in the CO-treated form of acetyl-CoA synthase, *Biochem.* **56**, 1248–1260 (2017).

[8] Huber, C. & Wächtershäuser, G. Activated acetic acid by carbon fixation on (Fe,Ni)S under primordial conditions. *Science* **276**, 245–247 (1997).

[9] Yamamoto, M. et al. Spontaneous and widespread electricity generation in natural deep-sea hydrothermal fields. *Angew. Chem. Int. Ed.* **56**, 5725–5728 (2017).

[10] Nakamura, R.; Takashima, T.; Kato, S.; Takai, K.; Yamamoto, M.; Hashimoto, K. Electrochemical current generation across a black smoker chimney. *Angew. Chem. Int. Ed.* **49**, 7692–7694 (2010).

[11] Ang, R. et al. Thermoelectricity generation and electron–magnon scattering in a natural chalcopyrite mineral from a deep-sea hydrothermal vent. *Angew. Chem. Int. Ed.* **54**, 12909–12913 (2015).

[12] Krissansen-Totton, J., Arney, G. N. & Catling, D. C. Constraining the climate and ocean pH of the early Earth with a geological carbon cycle model. *Proc. Natl. Acad. Sci. USA* **115**, 4105–4110 (2018).

[13] Yamaguchi, A. et al. Electrochemical $CO_2$ reduction by Ni-containing iron sulfides: How is $CO_2$ electrochemically reduced at bisulfide-bearing deep-sea hydrothermal precipitates? *Electrochim. Acta* **141**, 311–318 (2014).

[14] Ooka, H., McGlynn, S. E. & Nakamura, R. Electrochemistry at deep-sea hydrothermal vents: utilization of the thermodynamic driving force towards the autotrophic origin of life. *ChemElectroChem* **6**, 1316–1323 (2019).

[15] Kitadai, N. et al. Geoelectrochemical CO production: Implications of the autotrophic origin of life. *Sci. Adv.* **4**, eeao7265 (2018).

[16] Kitadai, N. et al. Metals likely promoted protometabolism in early ocean alkaline hydrothermal systems. *Sci. Adv.* **5**, eeav7848 (2019).

[17] Zhu, W. et al. Nickel sulfide microsphere film on Ni foam as an efficient bifunctional electrocatalyst for overall water splitting. *Chem. Commun.* **52**, 1486–1489 (2016).

[18] Xiao, H., Goddard III, W. A., Cheng, T. & Liu, Y. Cu metal embedded in oxidized matrix catalyst to promote $CO_2$ activation and CO dimerization for electrochemical reduction of $CO_2$. *Proc. Natl. Acad. Sci.* **114**, 6685–6688 (2017).

[19] Hori, Y. & Murata, A. Electrochemical evidence of intermediate formation of adsorbed CO in cathodic reduction of $CO_2$ at a nickel electrode. *Electrochim. Acta* **35**, 1777–1780 (1990).

[20] Hansen, H. A., Varley, J. B., Peterson, A. A. & Norskov, J. K. Understanding trends in the electrocatalytic activity of metals and enzymes for $CO_2$ reduction to CO. *J. Phys. Chem. Lett.* **4**, 388–392 (2013).

[21] Kondo, T. & Mitsudo, T. Metal-catalyzed carbon–sulfur bond formation. *Chem. Rev.* **100**, 3205–3220 (2000).

[22] Hirschbeck, V., Gehrtz, P. H. & Fleisher, I. Metal-catalyzed synthesis and use of thioesters: recent developments. *Chem. Eur. J.* **24**, 7092–7107 (2018).

[23] Pietrocola, F., Galluzzi, L., Pedro, J. M. B., Madeo, F. & Kroemer, G. Acetyl coenzyme A: A central metabolite and second messenger. *Cell Metabolism* **21**, 805–821 (2015).

[24] Satanowski A. & Bar-Even, A. A one-carbon path for fixing $CO_2$. *EMBO reports* **21**, e50273 (2020).

[25] Erley, W. & Wagner, H. Sulfur poisoning of carbon monoxide adsorption on Ni(111). *J. Catal.* **53**, 287–294 (1978).

[26] Ma, S. H., Jiao, Z. Y., Wang, T. X. & Zu, X. T. Effect of preadsorbed S on the adsorption of CO on Co(0001). *J. Phys. Chem.* **113**, 16210–16215 (2009).

[27] Chandru, K., Gilbert, A., Butch, C., Aono, M. & Cleaves II, H. J. The abiotic chemistry of tholated acetate derivatives and the origin of life. *Sci. Rep.* **6**, 29883 (2016).

[28] Lindahl, P. A. Acetyl-coenzyme A synthase: the case for a $Ni^0_p$-based mechanism of catalysis. *J. Biol. Inorg. Chem.* **9**, 516–524 (2004).

[29] Horn, B., Limberg, C. Herwig, C. & Mebs, S. (2011) The conversion of nickel-bound CO into an acetyl thioester: organometallic chemistry relevant to the acetyl coenzyme A synthase active site. *Angew. Chem. Int. Ed.* **50**, 12621–12625 (2011).

[30] Bekker, A. et al. Atmospheric sulfur in Archean komatiite-hosted nickel deposits. *Science* **326**, 1086–1089 (2009).

[31] Morrill, P. L. et al. Geochemistry and geobiology of a present-day serpentinization site in California: The Cedars. *Geochim. Cosmochim. Acta* **109**, 222–240 (2013).

[32] Tivey, M. K. Generation of seafloor hydrothermal vent fluids and associated mineral deposits. *Oceanography* **20**, 50–65 (2007).

[33] Heinen, W. & Lauwers, A. M. Organic sulfur compounds resulting from the interaction of iron sulfide, hydrogen sulfide and carbon dioxide in an anaerobic aqueous environment. *Orig. Life Evol. Biosph.* **26**, 131–150 (1996).

[34] Schulte, M. D. & Rogers, K. L. Thiols in hydrothermal solution: standard partial molal properties and their role in the organic geochemistry of hydrothermal environments. *Geochim. Cosmochim. Acta* **68**, 1087–1097 (2004).

[35] Baaske, P. et al. Extreme accumulation of nucleotides in simulated hydrothermal pore systems. *Proc. Natl. Acad. Sci.* **104**, 9346–9351 (2007).

[36] Benner, S. A. et al. When did life likely emerge on Earth in an RNA-first process? *ChemSystemsChem* **1**, e1900035 (2019).

[37] Weber, A. L. Nonenzymatic formation of "energy-rich" lactoyl and glyceroyl thioesters from glyceraldehyde and a thiol. *J. Mol. Evol.* **20**, 157–166 (1984).

[38] Chevallot-Beroux, E., Gorges, J. & Moran, J. Energy conservation via thioesters in a non-enzymatic metabolism-like reaction network. *ChemRxiv* (2019) DOI:10.26434/chemrxiv.8832425.

[39] Ragsdale, S. W. Life with carbon monoxide, *Crit. Rev. Biochem. Mol. Biol.* **39**, 165–195 (2004).

[40] Aono, M., Kitadai, N. & Oono, Y. A principled approach to the origin problem. *Orig. Life. Evol. Biopsh.* **45**, 327–338 (2015).

# Figures

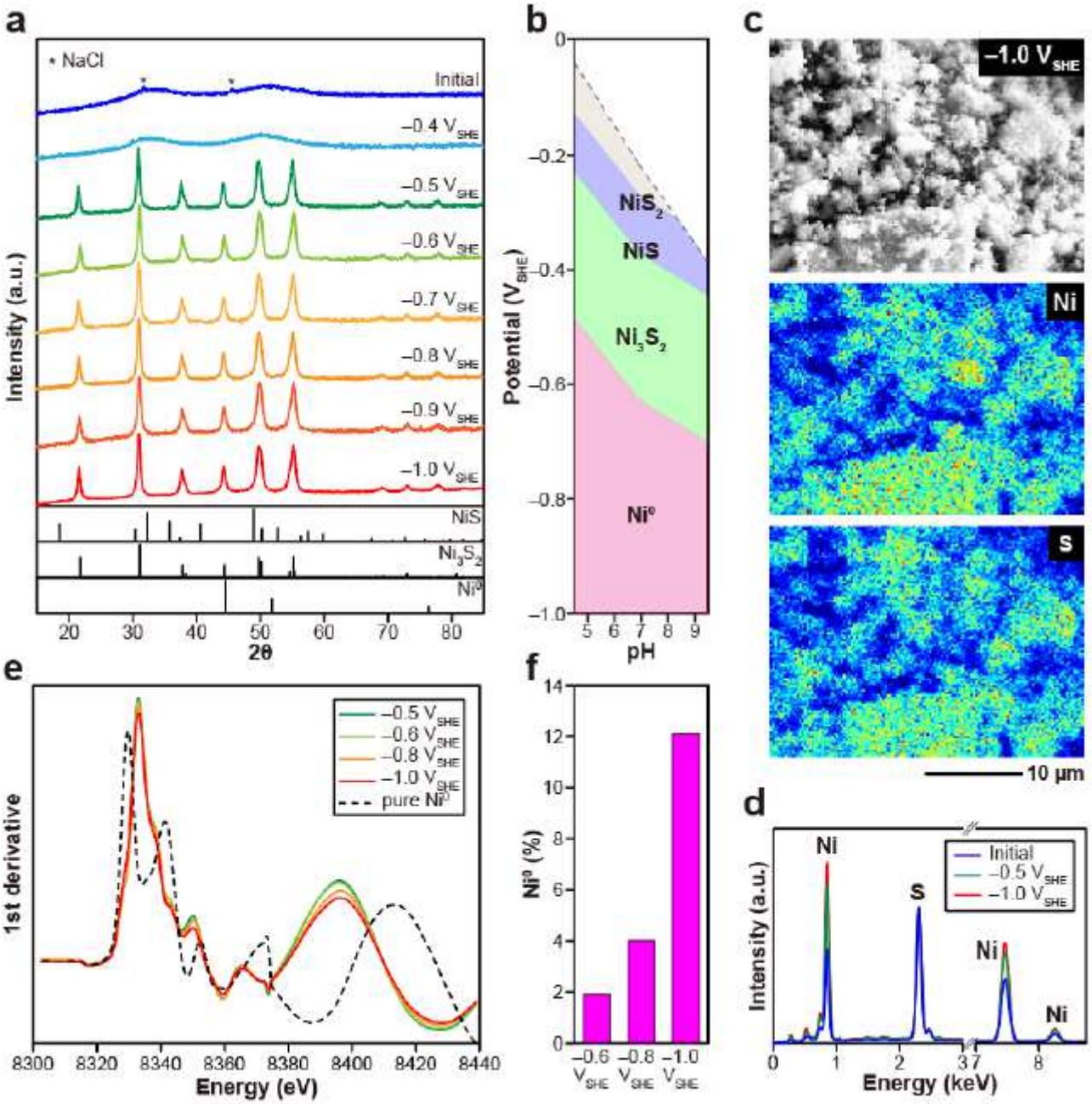


**Figure 1**

NiS electroreduction characterized by (a) XRD patterns, (b) thermodynamic calculation, (c and d) SEM-EDX mapping data, and (e and f) nickel K-edge XANES spectra. (c) presents the EDX mapping data for the NiS electrolyzed at −1.0 VSHE. In (d), the S signal intensities (2.3 keV) for NiS before (blue) and after the electrolysis at −0.5 VSHE (green) or −1.0 VSHE (red) are matched with each other for comparison. (e) The first derivative XANES spectra is shown.

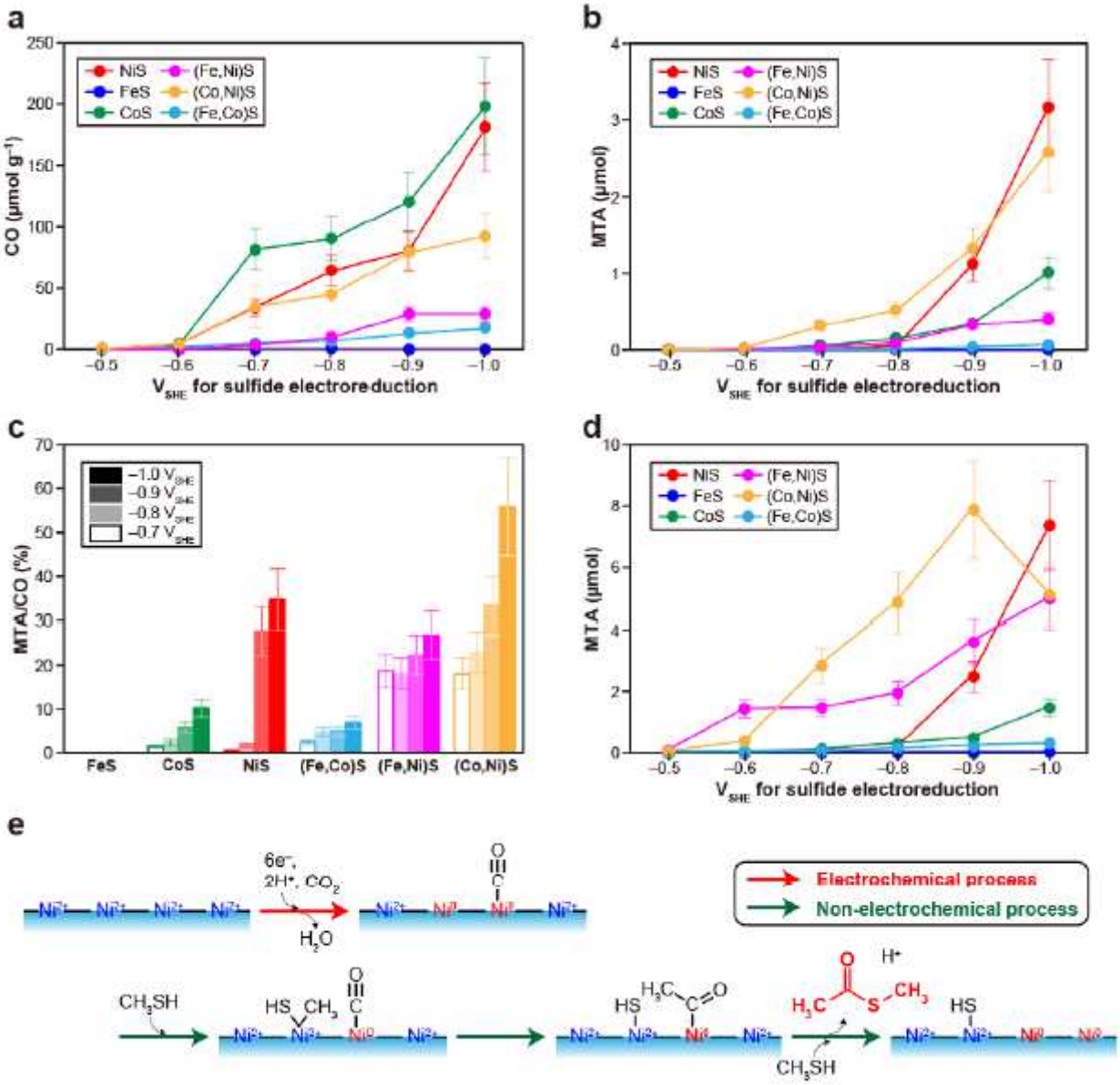


## Figure 2

CO accumulation through CO2 electroreduction (a) and CO conversion to S-methyl thioacetate (MTA) (b–d) on the metal-sulfide_PERMs. The surface-bound CO on the electrolyzed sulfides were quantified (a) and used as a carbon source for the MTA synthesis in the presence of methanethiol (75 μmol per 50 mg of sulfide) (b). The percentages of CO to form MTA are shown in (c). (d) The MTA synthesis were examined with CO and methanethiol externally added (75 μmol for each). The yield of MTA on (Co,Ni)S declined at the lowest potential (−1.0 VSHE) because of depletion of methanethiol (Table S4). (e) Possible intermediate steps in the MTA formation via the formation of NiS_PERM with the surface-bound CO (red arrow) and the CO-methanethiol reaction on NiS_PERM (green arrows).

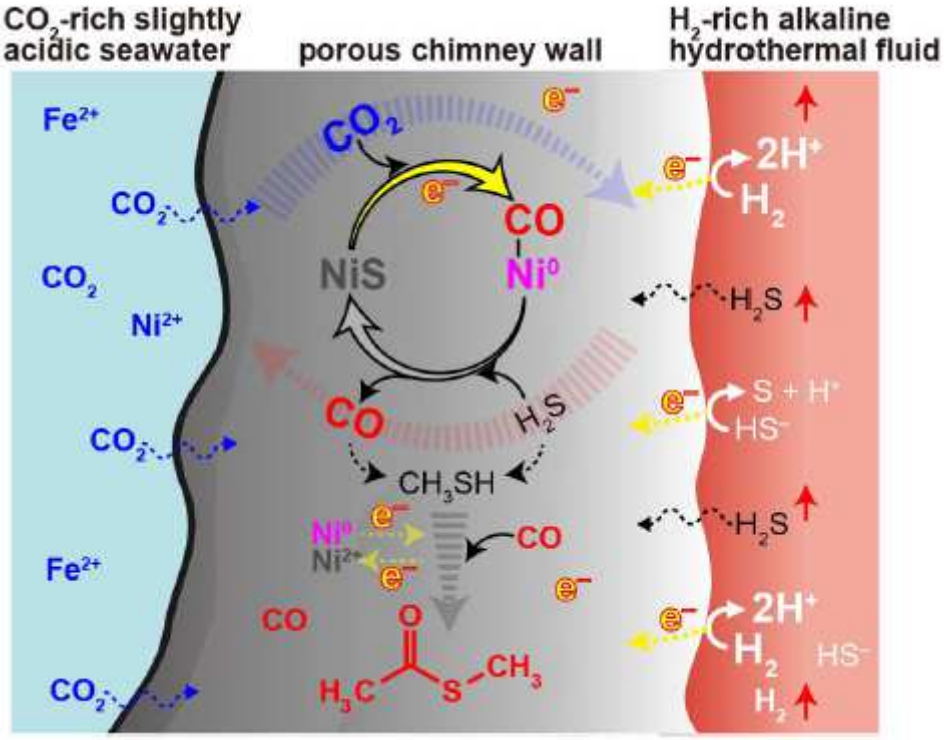


**Figure 3**

Schematic cross-section of a vent chimney in an early ocean alkaline hydrothermal system showing possible abiotic thioester synthesis promoted by Ni sulfide_PERM.

## Supplementary Files

This is a list of supplementary files associated with this preprint. Click to download.

- 200809MovieS1.mov
- 200824SupportingInformationCommunChem.pdf